Stimulated scattering of light in transparent particles. Influence of ponderomotive surface deformations

A.A. Zemlyanov, Yu.E. Geints, and A.V. Pal'chikov

Institute of Atmospheric Optics,
Siberian Branch of the Russian Academy of Sciences, Tomsk
Received February 16, 1999

We discuss here some peculiarities in the evolution of stimulated scattering in transparent liquid particles under the action of ponderomotive force induced by the light field. Strong deformations within the so-called Descartes ring are noticed that exceed deformations on the rest surface of a particle by an order of magnitude. The evolution dynamics of droplet deformations suggests that just these deformations are the main cause of the experimentally observed break of stimulated scattering. An analytical expression has been derived for the Q-factor of resonance eigenmodes caused by slight deviations of a droplet shape from a sphere. It is shown that a higher Q-factor experiences a stronger influence of the surface deformations.

Introduction

In recent years the interest in studies of the nonlinear effects of stimulated scattering (SRS, SBS, stimulated fluorescence) in microparticles has strongly increased. This is caused by a unique property of the dielectric spheres to accumulate and transfer the light wave energy. This property opens up wide possibilities for practical application of microparticles as independent optical devices in high-resolution spectroscopy,[1] optical communication,[2] remote analysis of chemical properties and microphysical parameters of aerosol.[3]

As known, the basic circumstance for stimulated scattering effects to occur in spherical microparticles is electromagnetic oscillation modes with a high Q-factor. Such modes are excited at certain values of the diffraction parameter $x = k_0 a_0$ (where a_0 is the particle radius, k_0 is the absolute value of the wave vector of a light wave in vacuum).[4] A transparent particle can actually be considered as an open spherical optical resonator having a set of resonance oscillation modes.

Spontaneous Raman scattering radiation generated at inelastic scattering of a pump wave in a particle volume may, under certain conditions, be "locked" by one (or several) resonance mode and amplified. As a result, a wave of stimulated scattering is formed in the spherical particle. The electromagnetic field of this wave is mostly concentrated in a thin layer near the particle surface.[5] From the viewpoint of wave optics, this field can be treated as a standing wave resulting from interference of two inelastically scattered waves, which are phase-matched and propagate from the opposite directions along the particle surface. Radiation loss of these waves through the particle surface gives rise to a particle glow at its edge. A frequency spectrum of this glow has a characteristic "peaked" structure, that reflects spectral positions of eigenmodes.[3,5]

At the same time, recent experimental investigations into the stimulated light scattering in liquid particles have revealed some peculiarities in the angular structure of the stimulated scattering flux.[6–11] In particular, it has been noted that the traditionally observed glow of the particle edge is accompanied by an intense glow at Raman frequencies from a ring area on the shadowed side of a particle. In Ref. 8 this zone has been called a Descartes ring (DR).

To explain this extra emission, Srivastava and Jamrzembski (Ref. 7) have put forward a hypothesis which implies that, in contrast to Raman emission due to tangential loss of the Stokes wave being in resonance, emission from DR is caused by high intensity of the inner pump field in this area, because the incident wave in DR is focused by the front surface of a spherical particle onto the shadowed hemisphere. Consequently, since the Raman scattering from DR is not related to particle's resonance properties, the spectral diagram of radiation from the ring area must be similar to that of stimulated scattering in a solid medium. As known, the latter is characterized by the absence of a peaked structure.[12]

However, further experimental studies[8–10] have shown that the spectral, temporal, and threshold characteristics of stimulated emission from the DR area have the same peculiarities as the radiation from the droplet edge. The authors of these papers have assumed that additional emission from the ring zone is caused by light scattering at nonlinear disturbances of the medium, which are caused by pump radiation in the areas of the maximum inner field.[9] These may be either processes leading to light-induced change of the refractive index of the particle's matter (Kerr effect, electrostriction) or surface distortions of a liquid particle induced by ponderomotive forces of the light field.[10] In our opinion, the latter mechanism is more probable, since up to date the scientific literature present no evidence on DR in solid spherical particles, which have a solid boundary. Thus, we can assume the following mechanism. The pump field induces strong deformations of the spherical surface in the DR zone. Electromagnetic waves of the resonance mode undergo scattering when incident on the drop portion distorted by the shape oscillations due to deformations. Thus the

0235-6880/99/05 398-08 $02.00 © 1999 Institute of Atmospheric Optics

appearance of an extra source of emission from a droplet may be explained. The presence of this emission indicates that deformations worsen resonance properties of a liquid particle, namely, decrease its Q-factor at the frequency of stimulated scattering.

This paper presents a study of changes in the radiation Q-factor of natural electromagnetic oscillations of a liquid particle due to surface deformations in the DR zone. This effect is estimated numerically based on calculations of ponderomotive oscillations of droplets in the field of an intense radiation. The results obtained have allowed interpretation of the experimental findings of Ref. 11 to be done. These data are interesting, in our opinion, since they imply a possibility of decreasing the power threshold of SRS in transparent droplets exposed to a wave train of picosecond laser pulses in the presence of ponderomotive effect of radiation upon the droplet surface.

Theory of formation of the Descartes ring

Rays, having experienced one refraction at the illuminated hemisphere of a spherical particle, form the area on its shadow side. The boundary of this area is called the Descartes ring.[8] The position of DR with respect to the principal cross section of a spherical particle illuminated by a plane electromagnetic wave can be found from considerations of geometrical optics. The geometry of DR formation is illustrated in Fig. 1, which shows the cross section of a spherical particle in the incidence plane of a light wave. The plane wave is incident on a water droplet along the direction of the z-axis. The angle φ_i is the impact parameter ($0 \le \varphi_i \le \pi/2$). It determines the position of the ray entrance point on the sphere as seen from its center. The angular position θ_i of the point of secondary refraction of the ith ray on the shadow side of the droplet is uniquely related to the angle φ_i by the Snell law:

$$\theta_i = 2\arcsin\,[(n_1/n_2)\,\sin\varphi_i] - \varphi_i, \qquad (1)$$

where n_1 and n_2 are the refractive indices of the ambient medium and the particle matter, respectively. Figure 2 shows the dependence $\theta_i(\varphi_i)$ for different refractive indices of a droplet matter.

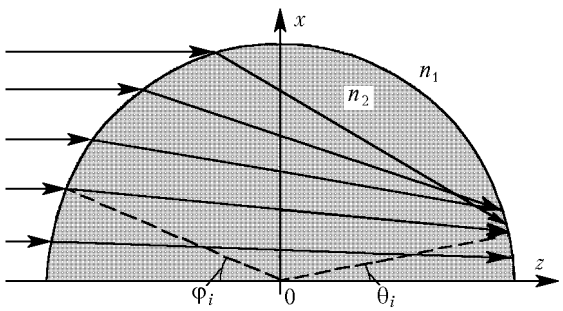

Fig. 1. Geometry of rays inside a spherical dielectric particle: the angular position, with respect to particle center, of the ith incident ray or the impact parameter (φ_i); the angular position of the second refraction of the ith ray (θ_i).

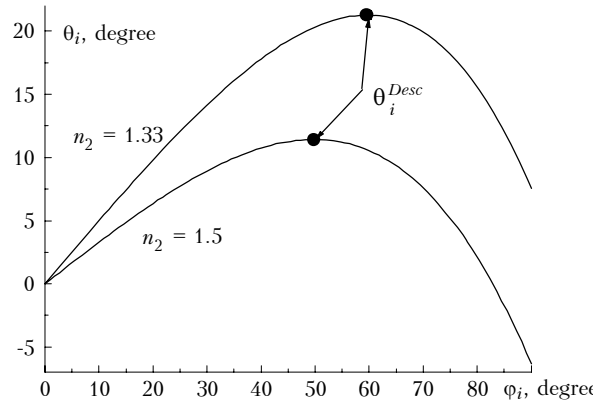

Fig. 2. The angular position of the secondary refraction point θ_i vs. impact parameter φ_i for particles with different refractive index n_2. The points show critical angles.

As seen, this dependence has a maximum θ_i^{Desc} at the impact parameter φ_i^{Desc}. The latter can be found from Eq. (1):

$$\varphi_i^{Desc} = \arctan\left(\sqrt{\frac{4n_1^2 - n_2^2}{n_2^2 - n_1^2}}\right).$$

The corresponding value of θ_i^{Desc} can be determined as

$$\theta_i^{Desc} = 2\arcsin\,[(n_1/n_2)\,\sin\varphi_i^{Desc}] - \varphi_i^{Desc}. \qquad (2)$$

The value of θ_i^{Desc} determines the critical angular size of DR on the shadow surface of the particle for rays, which have experienced one refraction.

As seen from Eq. (2), the angle θ_i^{Desc} is completely determined by the ratio of the refractive indices n_2/n_1. At $n_2/n_1 \ge 2$ the ring disappears.

The considerations based on the rigorous solution of the problem of a plane electromagnetic wave scattering on the sphere (Mie theory) give similar results. Figure 3 shows the numerically calculated distribution of the relative surface intensity of a light field $B(r, \theta, \varphi)$ in the DR zone for droplets of different liquids with radius a_0 = 40 μm, where

$$B(r, \theta, \varphi) = [E(r, \theta, \varphi)\,E^*(r, \theta, \varphi)]/E_0^2;$$

E_0 and E are the strength of electric fields of incident wave and the wave inside the particle; r, θ, and φ are the spherical coordinates. It is seen from Fig. 3 that the maxima of surface intensity of the light field, for example, for water are observed, on the shadow hemisphere of the droplet, at the points shifted by about 20° from the principal axis. They form a ring with the position coinciding with that obtained within the geometric optics approximation. For liquid particles with higher refractive index (benzene, CS_2) the position of the ring also coincides with that predicted by geometric optics. However, in this case, an additional maximum of the surface intensity is observed at the center of the shadow side of the droplet, in spite

of edge maxima. The amplitude of this maximum is practically equal to the amplitude observed in the ring zone (benzene) or even exceeds it (CS_2).

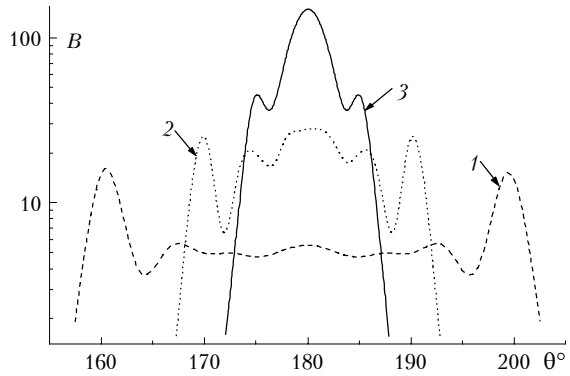

Fig. 3. Angular distribution of the relative surface intensity of a light field B near the center of the shadow hemisphere of a droplet ($\theta = 180°$) for different droplet matter: water (*1*), benzene (*2*), CS_2 (*3*).

Ponderomotive deformations of the droplet surface in the zone of the Descartes ring

The ponderomotive effect occurs in a liquid dielectric particle when it is exposed to high-intensity laser radiation. This effect causes appearance of a volume gradient of the liquid density (the striction effect), motion of the particle as a whole under the action of light pressure, as well as particle deformation due to surface forces. The latter physical mechanism is associated with a sharp change of the normal component of the electric field strength at the "liquid–ambient medium" interface. It is just this effect that makes up the subject of our further considerations.

The statement of the problem on deformation of a liquid droplet in a light field traditionally involves the equations of viscous incompressible liquid, as well as the kinematic and dynamic conditions on a free surface.[13,14] The former condition relates the deformation vector and the liquid flow velocity, while the latter one presents the strength balance on the particle surface:

$$\left\{p - \frac{\rho}{8\pi}\frac{\partial\varepsilon_2}{\partial\rho}E^2 - p_a - \alpha\left(\frac{1}{R_1}+\frac{1}{R_2}\right) + f\right\} n_i = \eta\left(\frac{\partial v_i}{\partial x_k}+\frac{\partial v_k}{\partial x_i}\right) n_k, \qquad (3)$$

where v, p, ρ, and η are the velocity, pressure, density, and dynamic viscosity of the liquid, respectively ; ε_2 is the liquid dielectric constant; p_a is the outer (atmospheric) pressure; α is the surface tension coefficient of the liquid; R_1 and R_2 are the principal radii of curvature of the surface; $\mathbf{n}$ is the unit vector of the normal to the droplet surface; $n_{i,k}$ is its projection onto the $x_{i,k}$ coordinate axes;

$$f = (\varepsilon_2 - 1)\,[(\varepsilon_2 - 1)\,(\mathbf{En})^2 + E^2]/8\pi \qquad (4)$$

is the change of the normal component of electromagnetic field strength on the liquid surface.[15] Only low-frequency (with respect to the frequency of exciting radiation) terms should be taken into account in Eqs. (3) and (4).

To derive the equation for oscillations of a liquid particle, let us use the approach developed in Ref. 16. This approach is based on the integral form of the law of energy conservation as applied to the liquid in a deformed particle. As known, change in the kinetic energy of a liquid in the field of body forces is described by the expression[13,14]:

$$\frac{\partial}{\partial t}\int_V \frac{\rho\, v^2}{2}\,\mathrm{d}V = -\int_S\left[\rho\mathbf{v}\left(\frac{v^2}{2}+\frac{p}{\rho}\right) - (\mathbf{v}\,\sigma)\right]\mathrm{d}\mathbf{S} - \int_V \sigma_{ik}\frac{\partial v_i}{\partial x_k}\,\mathrm{d}V + \int_V \mathbf{f}_E\,\mathbf{v}\,\mathrm{d}V, \qquad (5)$$

where σ_{ik} is the viscous stress tensor; V is the volume; S is the distorted surface of the liquid; $\mathrm{d}\mathbf{S} = \mathbf{n}\,\mathrm{d}S$; $\mathbf{f}_E$ is the volume density of ponderomotive forces.[15]

In what follows, we use the approximation of small deformations of the droplet surface and low viscosity of the liquid. The condition of small deformations means that $|\xi| / |\mathbf{r}_0| = |\mathbf{r} - \mathbf{r}_0| / |\mathbf{r}_0| \ll 1$, where $\mathbf{r}_0$ is the vector of a point on the undistorted droplet surface; ξ is the surface displacement vector. In the approximation of low viscosity, the flow inside the droplet can be considered potential ($\nabla \times \mathbf{v} = 0$). The only exception is the boundary layer with the thickness $l_b \sim a_0\,(\mathrm{Re})^{-1/2}$, where Re is Reynolds number.[13] When used together, these approximations guarantee correct calculation of the surface integral in Eq. (5).

The amplitude of the particle surface deformation can be written as a series in terms of spherical harmonics $(r/a_0)^l\, Y_{ln}(\theta, \varphi)$:

$$\xi(r, \theta, \varphi) = \sum_{ln} \xi_{ln}\,(r/a_0)^l\, Y_{ln}(\theta, \varphi),$$

where $Y_{ln}(\theta, \varphi)$ is the spherical harmonic. Thus, within the scope of the assumptions accepted and with regard for the boundary condition (3), we have from Eq. (5) that

$$\frac{\mathrm{d}^2\,\xi_{ln}}{\mathrm{d}t^2} + \frac{2}{t_l}\frac{\mathrm{d}\xi_{ln}}{\mathrm{d}t} + \Omega_l^2\,\xi_{ln} = \frac{l\, f_{ln}(t)}{a_0\,\rho}, \qquad (6)$$

where

$$f_{ln} = \int_0^{2\pi}\mathrm{d}\varphi\int_0^{\pi} f(t, r_0)\; Y_{ln}^*(\theta,\varphi)\,\sin\theta\,\mathrm{d}\theta;$$

$$t_l = \frac{a_0^2}{2\nu\,(2l+1)\,(l-1)}$$

is the characteristic time of oscillation damping due to viscosity;

$$\Omega_l = \sqrt{l(l-1)\,(l+2)\,\alpha/(\rho a_0^3)}$$

is the natural (Rayleigh) frequency of hydrodynamic oscillations of the droplet; $\nu = \eta/\rho$ is the kinematic viscosity of the liquid.

Given known form of the function $f(\mathbf{r}, t)$, Eq. (6) can be solved by use of standard procedures of numerical differentiation.

Figure 4 shows the surface shape for droplets of different liquids at a fixed time. The shape is distorted by ponderomotive deformations. The relative amplitude of deformations ξ/a_0 is shown in Fig. 5 as a function of the polar angle θ. The calculations have been performed with the following initial parameters: the particle is exposed to a pulsed laser radiation with pulse peak intensity $I_0 = 0.1$ GW/cm^2, pulse duration $t_p = 100$ ps, and the pulse sequence period $\tau = 13.2$ ns, at the wavelength $\lambda = 0.532$ μm. These parameters correspond to the data from Ref. 10. The shape of surface deformations is shown at the time, when the second laser pulse in the train begins to act upon the particle, that is, 13.2 ns after the beginning of the interaction.

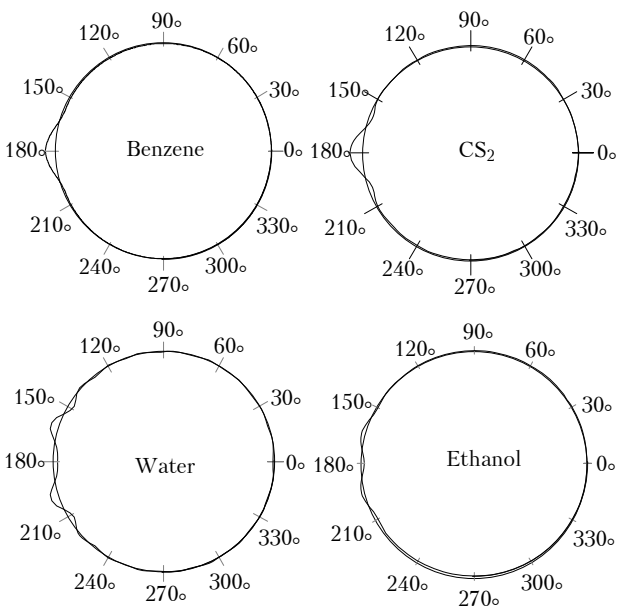

Fig. 4. The shape of the distorted surface of droplets of different liquids (the radiation is incident from right to the left). Deformations are shown schematically on a larger scale.

Strong deformations in the DR zone are clearly seen for a water droplet at the angles θ ≈ 160 and 200°. This coincides with the DR position for the parameter $n_2/n_1 = 1.33$ (see Fig. 3) and corresponds to the angular displacement of ~ 20° from the principal axis. The amplitude of deformations in this area is an order of magnitude larger than displacements in the rest of the droplet surface.

For the benzene particle ($n_2 \approx 1.5$), the area of deformations is a single convexity in the direction of the principal axis, rather than a ring. The height of this convexity exceeds the amplitude of deformations on the rest of the particle surface by more than 20 times. The explanation is as follows. The maximum of the electromagnetic field at the shadow side of the benzene droplet is closer to the center as compared to water droplets. The size of the zone of maximum light field intensity is about 10° in this case, and DR degenerates into a spot because of the higher light intensity in this area (see Fig. 3). Similar regularity in the spatial pattern of stimulated scattering emission has also been noticed in Ref. 10. Chen et al.[10] reported about additional emission from the point area on the shadow side of a droplet for liquid particles of CS_2 with the refractive index exceeding that of water.

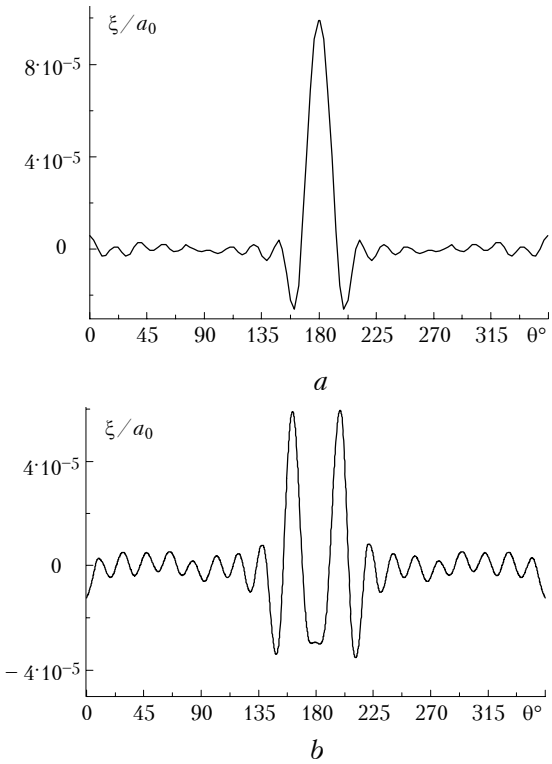

Fig. 5. The relative amplitude of surface deformations caused by the ponderomotive forces for the droplet with radius $a_0 = 40$ μm vs. polar angle θ: benzene (*a*), water (*b*).

Experimental research into the action of a series of short laser pulses ($t_p = 100$ ps) on transparent droplets has also revealed some interesting peculiarities in the temporal structure of SRS signals.[11] It was found that at such a sequence of exciting pulses it is possible to decrease the energy threshold of SRS. An individual radiation pulse in a train does not give rise to SRS signal. At the same time, on passage of some number of laser pulses, stimulated Raman scattering from liquid particles occurs. Besides, the SRS has been observed only in a certain time interval. It was found that the

length of this interval depends on the pump pulse intensity. This dependence is illustrated in Fig. 6, where the irradiation intensity is shown in percent of some threshold intensity $I_0 = 30$ GW/cm^2. By the threshold intensity in Ref. 11 is meant the peak intensity of a pump pulse, when a single pulse is sufficient for generating the SRS. Open circles in Fig. 6 are for the time, when SRS signal occurs in droplets. The squares are for the time, when emission at the SRS frequency from particles terminates. Curves in Fig. 6 show the time zone, within which laser pump pulses lead to SRS generation in droplets.

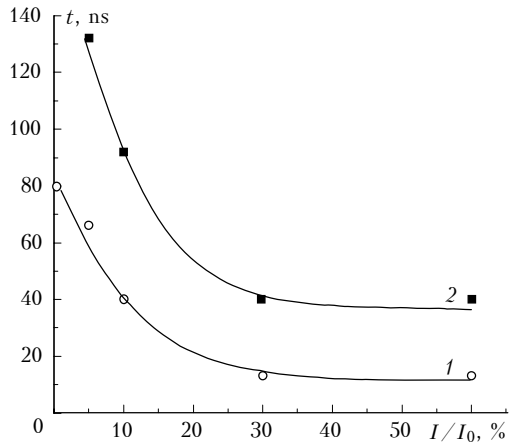

Fig. 6. Time of start and termination of the SRS signal generation in ethanol droplets as a function of the relative peak intensity of a pump pulse $I/I_0 \cdot 100\%$. The experimental data have been borrowed from Ref. 11. Open circles correspond to the start of SRS signal generation; squares correspond to the termination of SRS signal generation. Curves *1* and *2* are the borders of the time zone, within which the SRS generation occurs.

In our opinion, this time zone is most likely caused by local deformations of the particle surface. The deformations are induced by the ponderomotive forces in the areas of maximum light field on the particle surface (DR zone). As shown above, these deformations lead to distortions of the spherical surface of a droplet and formation of peaks and dips on it. These peaks and dips are responsible for a peculiar kind of selection among the resonance electromagnetic modes, which sustain the process of stimulated scattering. In an ideal sphere the oscillations with higher Q-factor apparently dominate in the competition between the resonance modes, all other factors being the same. Since typical values of the radiation Q-factor for large dielectric spheres (with the diffraction parameter $x > 100$) are on the order of $Q_R \geq 10^{10}$ (see, for example, Ref. 17), the effective Q-factor for natural oscillations is completely determined by the absorption losses in a liquid Q_A: $1/Q = 1/Q_A + 1/Q_R$. Therefore, if the pump pulse length t_p is shorter than the characteristic locking time of SRS radiation in the resonator τ_R ($\tau_R \sim 1/Q_R$), then the radiation of this mode practically cannot leave the droplet and is completely absorbed.

The situation is quite different for the case of surface deformations of a liquid particle. In this case, modes, for which the Q-factor is lower, while being more stable to deformations of the resonator surface have an advantage, because the electromagnetic field of this modes is concentrated farther from the surface.[4] Because radiation loss of these modes is higher, the most part of radiation leaves the particle, and the particle starts to glow. However, as the process of droplet deformation evolves, the spatial structure of resonance modes becomes so distorted that they are incapable of sustaining the nonlinear scattering process. As a result, some time later the generation terminates.

This theoretical model of light-induced deformations of a liquid particle has provided the basis for our numerical experiments. In this experiments we have related the SRS time zone shown in Fig. 6 to the corresponding amplitudes of deformation of the droplet surface in the DR area. The calculated results are shown in Fig. 7. Two curves mark the amplitude range of particle deformations, within which the SRS generation occurs. As seen from the figure, the amplitude of surface deformations increases by an order of magnitude during the time of SRS existence. This amplitude far exceeds the level of natural thermocapillary oscillations of the droplet (dashed line in Fig. 7). The characteristic amplitude of the latter oscillations can be presented as[18]:

$$|\xi_{t.c.}| = \sqrt{k_B T/(4\pi\alpha)},$$

where k_B is the Boltzmann constant; T is the temperature of the particle.

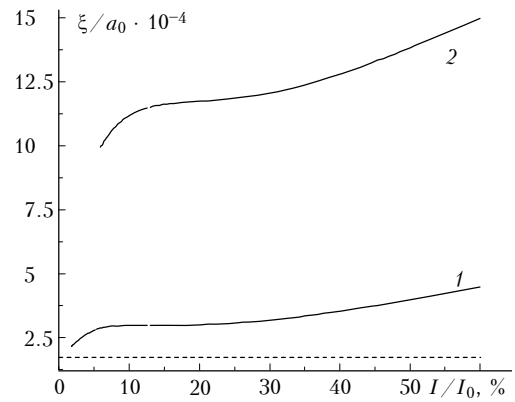

Fig. 7. Numerically calculated dependence of the relative amplitude of ponderomotive deformations of an ethanol droplet ($a_0 = 40$ μm) on the relative peak intensity of the pump pulse: beginning of the SRS generation (curve *1*); termination of the SRS generation (curve *2*). The data for calculations have been taken from Fig. 6. The dashed straight line is for the rms amplitude of the thermocapillary oscillations of the liquid.

Thus, the results presented allow the following conclusions to be drawn. In the DR area there occur sharp deformations of the surface of a transparent droplet. These deformations are caused by the action of ponderomotive forces in a high-intensity light field. At

the refractive index $n_2 = 1.33$ (water) and $n_2 = 1.36$ (ethanol), the area of deformations has a ring shape. For liquid droplets with higher refractive index $n_2 > 1.4$ (benzene, CS_2) the ring takes the form of a spot at the center of the shadow surface of a droplet. The amplitude of these deformations exceeds the amplitude of deformations on the rest surface of the particle by more than an order of magnitude. Consequently, these deformations can cause additional emission of SRS radiation from the DR area.

Influence of the surface deformations of a liquid droplet on the *Q*-factor of the resonance natural modes

To estimate the influence of surface deformations of droplets on the Q-factor of the resonance modes, we proceed from the traditional concept of the resonance mode as a standing wave, whose field is localized mostly in the plane passing through the center of the sphere being inclined at an angle θ_{lm} to the z-axis (Fig. 8) (Ref. 5). This angle is determined by the ratio of the azimuth index of the resonance mode m to its number l: $\theta_{lm} = \arccos(m/l)$. Since the index m varies within the range $(l; -l)$, the plane of a circle, where the mode field is mostly localized, lies at the polar angles $\theta = 0 - \pi/2$.

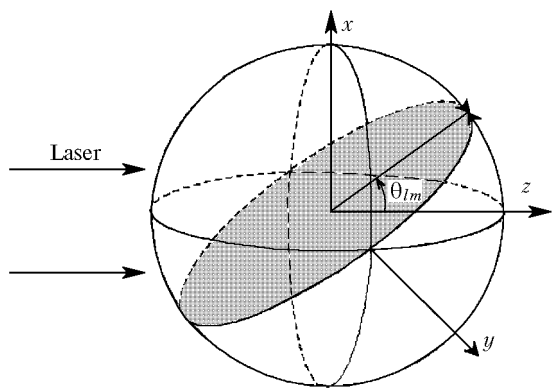

Fig. 8. The field of the resonance mode with the azimuth index m. The electromagnetic field is localized in the ring zone inclined at the angle θ_{lm} relative to the equator.

A standing wave is formed by traveling waves that arrive at the initial point with the phases multiple of 2π. That means that the condition of phase matching must hold: $ka_0 = l$, where k is the wave number inside a droplet. Consequently, to keep the phase matching, any surface deformations, which change the traveling wave path length by δL, should be compensated for by the corresponding change in the absolute value of the wave vector δk: $\delta L/L_0 = \delta k/k$, where $L_0 = 2\pi a_0$ is the geometrical length of the wave travel path in an ideal sphere.

For the length increment we can obtain

$$\delta L \cong \frac{2\pi a_0}{\pi - 2\theta_{lm}} \int_{\theta_{lm}}^{\pi-\theta_{lm}} \xi(\theta)\mathrm{d}\theta =$$

$$= \xi_A \frac{2\pi a_0}{\pi - 2\theta_{lm}} \int_{\theta_{lm}}^{\pi-\theta_{lm}} \bar{\xi}(\theta)\mathrm{d}\theta,$$

where ξ_A is the amplitude of surface deformations, $\bar{\xi} = \xi(\theta)/\xi_A$.

In the first approximation ($\xi_A \ll 1$), we can consider the shape of the deformed principal cross section of a particle as a circle with some effective radius a_e depending on the amplitude and angular structure of the deformations:

$$a_e = (L_0 + \delta L) = a_0\,(1 + \xi_A q_{lm}).$$

Here $q_{lm} = \frac{1}{\pi - 2\theta_{lm}} \int_{\theta_{lm}}^{\pi-\theta_{lm}} \bar{\xi}(\theta)\mathrm{d}\theta$ is the transformation coefficient (obviously, $|q_{lm}| \le 1$). Then, for the change in the diffraction parameter of the effective sphere δx for the $\mathrm{TE(TM)}_{lm}$ mode, we have the following expression:

$$\delta x = x_e - x_0 = \frac{\delta k}{n_2}\, a_0 = x_0\, \xi_A\, q_{lm}, \qquad (7)$$

where x_0 is the resonance value of the diffraction parameter of the undistorted sphere, $x_e = k_0 a_e$.

The dependence of q_{lm} on m/l in liquid particles deformed in accordance with Fig. 5 is shown in Fig. 9. It is seen that the values of q_{lm} vary within $10^{-3} - 10^{-2}$ and reach maximum for the modes lying in the plane of the droplet equator ($m = l$).

As calculations show, the shape of the resonance curve of the particle natural modes is close to the Lorentzian profile.[19] Therefore, in the immediate vicinity of some resonance, we can introduce the so-called Q-factor function:

$$Q_D(x_0) = Q_0/[1 + (x_e - x_0)^2/\Delta x^2],$$

where Q_0 is the Q-factor of some resonance mode of an undistorted sphere (the mode indices are omitted for simplicity); Δx is the half-width of the resonance curve. The value of this function at $x_e = x_0$ obviously coincides with the resonance Q-factor. By making use of Eq. (7) and taking into account that $Q_0 = x_0/\Delta x$, we have

$$Q_D(x_0) = Q_0/[1 + (q_{lm}\,\xi\, Q_0)^2]. \qquad (8)$$

Figure 10 shows the dependence of Q_D on Q_0 for different values of the surface deformations ξ_A. The values are taken from Fig. 7. The value of the coefficient q_{lm} was set parametrically in the range $|q_{lm}| \sim 10^{-3}$–10^{-1}. As follows from this figure, the higher Q_0 value, the stronger the effect of deformations on the Q-factor of the resonance modes.

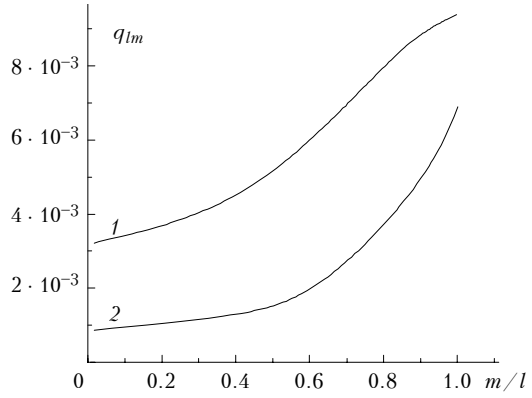

Fig. 9. The transformation coefficient q_{lm} as a function of the parameter m/l for the droplet deformations as in Fig. 5: water (curve *1*), CS_2 (curve *2*).

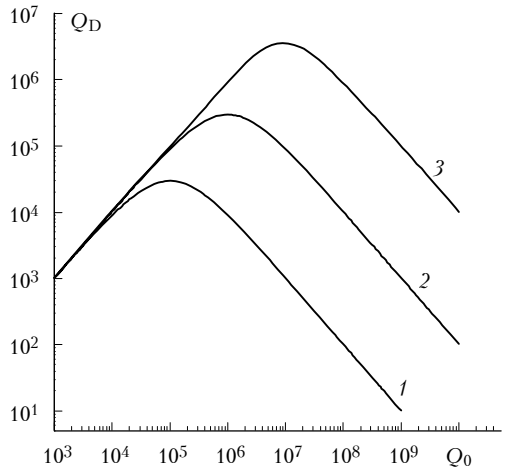

Fig. 10. Q-factor of the deformed droplet Q_D as a function of the Q-factor of an ideal sphere Q_0 at different values of the parameter $q_{lm}\xi/a_0$: 10^{-1} (*1*); 10^{-2} (*2*); 10^{-3} (*3*).

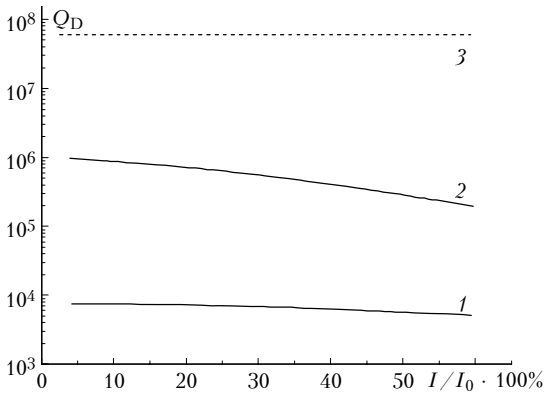

Fig. 11. Q-factor of the deformed ethanol droplets vs. relative peak intensity of a pump pulse according to the results of numerical experiment (the initial data were borrowed from Ref. 11): beginning of the SRS generation (*1*); termination of the SRS generation (*2*); the dashed straight line shows the limit for the Q-factor caused by the thermocapillary deformations.

The results presented allow us to relate the values of ethanol droplet deformations (see Fig. 7) to the changes of the radiation Q-factor at different peak intensity of a pulse of incident radiation. The changes can be calculated by Eq. (8). The obtained dependence is shown in Fig. 11. It follows from this figure, that as the pump pulse intensity increases, the threshold value of the Q-factor, at which the SRS signal occurs, decreases by about a factor of three. At the same time, the boundary value of Q_D, which corresponds to the SRS termination, remains practically unchanged. In other words, resonance modes having the Q-factor below some threshold value $Q_D \sim 8 \cdot 10^3$ are incapable of sustaining the process of stimulated scattering no matter what is the intensity of the pump radiation.

Conclusion

In this paper we have considered some peculiarities in the evolution of the process of stimulated scattering in transparent liquid particles under the action of ponderomotive forces induced by the light field. Appearance of strong deformations in the DR area has been noticed. These deformations exceed deformations of the rest of the droplet surface by more than an order of magnitude.

Studies of the evolution dynamics of droplet deformations have shown that these deformations can be considered as the main reason for break of the SRS generation, which has been observed in experiments. The analytical expression has been obtained to estimate a decrease in the Q-factor of natural resonance modes due to slight deviations of the particle shape from the sphere. It is shown that the higher Q-factors of the droplet's resonance modes take place under stronger effect of the surface deformations. The level of pump intensity itself is the factor, which performs an effective selection among the resonance modes at their competition to sustain the process of stimulated scattering in transparent particles.

References

1. A.S. Kwok and R.K. Chang, Optics & Photonics News **4**, No. 12, 34 (1993).
2. B. Little, H. Haus, E. Ippen, G. Steinmeyer, and E. Thoen, Optics & Photonics News **9**, No. 12, 32–33 (1998).
3. G. Schweiger, J. Aerosol Sci. **21**, No. 4, 483–509 (1990).
4. Yu.E. Geints and A.A. Zemlyanov, Atmos. Oceanic Opt. **9**, No. 10, 854–858 (1996).
5. R.K. Chang and A.J. Campillo, *Optical Processes in Microcavities* (World Scientific Publ. Co., Singapore, 1996).
6. M.A. Jarzembski and V. Srivastava, Appl. Opt. **28**, No. 23, 4962–4965 (1989).
7. V. Srivastava and M.A. Jarzembski, Opt. Lett. **16**, No. 3, 126–128 (1991).
8. J.G. Xie, T.E. Ruekgauer, J. Gu, R.L. Armstrong, and R.G. Pinnick, Opt. Lett. **16**, No. 17, 1310–1312 (1991).

9. J.G. Xie, T.E. Ruekgauer, J. Gu, R.L. Armstrong, R.G. Pinnick, and J.D. Pendleton, Opt. Lett. **16**, No. 23, 1817–1819 (1991).
10. G. Chen, D.Q. Chowdhury, R.K. Chang, and W.-F. Hsieh, J. Opt. Soc. Am. B **10**, No. 4, 620–632 (1993).
11. J.M. Hartings, X. Pu, J.L. Cheung, and R.K. Chang, J. Opt. Soc. Am. B **14**, No. 11, 2842–2849 (1997).
12. l .l . Sushchinskii, *Stimulated Scattering of Light* (Nauka, Moscow, 1985), 175 pp.
13. A.A. Zemlyanov, Kvant. Elektron. **1**, 2085–2088 (1974).
14. L.D. Landau and E.M. Lifshits, *Fluid Mechanics* (Pergamon Press, Oxford, 1969).
15. L.D. Landau and E.M. Lifshits, *Electrodynamics of Continuous Media* (Pergamon Press, Oxford, 1974).
16. Yu..E. Geints and A.A. Zemlyanov, Atmos. Oceanic Opt. **10**, Nos. 4–5, 313–321 (1997).
17. L.A. Vainshtein, *Open Resonators and Open Wave Guides* (Sov. Radio, Moscow, 1966), 476 pp.
18. H.M. Lai, P.T. Leung, and K. Young, Phys. Rev. A **41**, No. 9, 5199–5204 (1990).
19. Yu.E. Geints, A.A. Zemlyanov, and A.V. Pal'chikov, Atmos. Oceanic Opt. **10**, No. 12, 974–978 (1997).